

An efficient feature selection and explainable classification method for EEG-based epileptic seizure detection

Ijaz Ahmad ^{a,b,c,1}, Chen Yao ^{d,1}, Lin Li ^e, Yan Chen ^e, Zhenzhen Liu ^e, Inam Ullah ^f, Mohammad Shabaz ^g, Xin Wang ^{a,b,c}, Kaiyang Huang ^h, Guanglin Li ^{a,c}, Guoru Zhao ^{a,c,*}, Oluwarotimi Williams Samuel ^{i,j,*}, Shixiong Chen ^{a,c,*}

^a CAS Key Laboratory of Human-Machine Intelligence Synergy Systems, Shenzhen Institute of Advanced Technology, Chinese Academy of Sciences, Shenzhen, Guangdong 518055, China

^b Shenzhen College of Advanced Technology, University of Chinese Academy of Sciences, Shenzhen, Guangdong 518055, China

^c Guangdong-Hong Kong-Macao Joint Laboratory of Human-Machine Intelligence-Synergy Systems, Shenzhen, Guangdong 518055, China

^d Department of Neurosurgery, The National Key Clinic Specialty, Shenzhen Key Laboratory of Neurosurgery, the First Affiliated Hospital of Shenzhen University, Shenzhen Second People's Hospital, 3002 # Sungang Road, Futian District, Shenzhen, Guangdong 518055, China

^e Surgery Division, Epilepsy Center, Shenzhen Children's Hospital, Shenzhen, Guangdong 518055, China

^f Department of Computer Engineering, Gachon University, Seongnam 13120, Republic of Korea

^g Model Institute of Engineering and Technology, Jammu, J&K, India

^h Medical Information Engineering, Guangzhou University of Chinese Medicine, Guangzhou 510405, China

ⁱ School of Computing, University of Derby, Derby, DE22 3AW, United Kingdom

^j Data Science Research Centre, University of Derby, Derby, DE22 3AW, United Kingdom

ARTICLE INFO

Keywords:

Electroencephalogram

Machine learning

Coefficient correlation

Distance correlation

Biomedical signals

Explainable artificial intelligence

ABSTRACT

Epilepsy is a prevalent neurological disorder that poses life-threatening emergencies. Early electroencephalogram (EEG) seizure detection can mitigate the risks and aid in the treatment of patients with epilepsy. EEG based epileptic seizure (ES) detection has significant applications in epilepsy treatment and medical diagnosis. Therefore, this paper presents an innovative framework for efficient ES detection, providing coefficient and distance correlation feature selection algorithms, a Bagged Tree-based classifier (BTBC), and Explainable Artificial Intelligence (XAI). Initially, the Butterworth filter is employed to eliminate various artifacts, and the discrete wavelet transform (DWT) is used to decompose the EEG signals and extract various eigenvalue features of the statistical time domain (STD) as linear and Fractal dimension-based non-linear (FD-NL). The optimal features are then identified through correlation coefficients with *P*-value and distance correlation analysis. These features are subsequently utilized by the Bagged Tree-based classifier (BTBC). The proposed model provides best performance in mitigating overfitting issues and improves the average accuracy by 2% using (CD, E), (AB, CD, E), and (A, B) experimental types as compared to other machine learning (ML) models using well-known Bonn and UCI-EEG benchmark datasets. Finally, SHapley additive exPlanation (SHAP) was used to interpret and explain the decision-making process of the proposed model. The results highlight the framework's capability to accurately classify ES, thereby improving the diagnosis process in patients with brain dysfunctions.

1. Introduction

Epilepsy is a noncontagious brain disorder that develops from irregular electrical brain activity [1,2]. A delay in the diagnosis process can create severe mental health problems or even lead to death [3]. Globally, over sixty million people have been affected by the epilepsy disease reported by the World Health Organization (WHO) [4]. In order to mitigate the progression of the disease, the early diagnosis and

detection of epileptic seizures (ES) are crucial. Recently, various diagnostic approaches have captured the attention of specialized medical professionals for the diagnosis of epilepsy [5]. Moreover, neurologists recommended electroencephalography (EEG) to monitor the brain electrical activity of the seizure [6]. Conventional epilepsy diagnosis in clinical settings involves specialists visually inspecting during EEG

* Corresponding author at: Shenzhen College of Advanced Technology, University of Chinese Academy of Sciences, Shenzhen, Guangdong 518055, China.
E-mail address: sx.chen@siat.ac.cn (S. Chen).

¹ The first two authors contributed equally to this work.

recordings, which is laborious and intensive work [7,8]. Therefore, Machine Learning (ML) models have been introduced for efficient analysis by classifying EEG signals [8]. Moreover, existing automated EEG ES detection approaches are often less used in real-time clinical applications because of their low sensitivity and specificity in clinical epilepsy management. Several challenges exist in the automation of EEG ES detection. Primarily, the extraction of highly representative features is challenging because of the nonlinear and non-stationary nature of EEG signals [8]. Secondly, the selection of the optimal features from EEG pattern, which poses efficient features to identify the differentiation between pre-ictal and seizure state. The third challenge pertains to minimizing the miss classification rate, arising from the similarities in oscillatory and fractal characteristics across seizure and non-seizure EEG signals [7]. The fourth challenge includes the interoperability and explainability of the ML model, which are essential for informed clinical decisions and enhancing patient safety. To address the above informative challenges, this study presents a novel framework for the efficient detection of EEG ES utilizing biomedical EEG signals. The framework consists of a feature extraction method that exploits distinctive FD-nonlinear (FD-NL) and statistical time domain (STD) features extracted from decomposed EEG signal sub-bands, capturing the EEG signals' nonlinear and time-domain information. The proposed study also employs correlation coefficients (CC) for linear feature selection and distance correlation (DC) for non-linear feature selection in EEG ES detection. Additionally, the proposed study employs a Bagged Tree-based classifier to enhance the accuracy of ES classification. Moreover, the use of explainable AI (XAI) interpret the decision-making process behind the model's detection. XAI facilitates a transparent and understandable explanation of ML model or algorithm decisions [9,10], which is especially important in ES detection by providing clinicians insights into the decision-making process. The proposed framework, with the integration of XAI, aims to enhance the diagnostic decision-making process in clinical practice. The proposed study is summarized as follows:

- The splitting and decomposition of EEG signals is performed by Discrete Wavelet Transform (DWT). From the different decomposition levels, the statistical time domain as linear and Fractal dimension-based non-linear features are extracted.
- Applied Correlation Coefficients and Distance Correlation feature selection methods to select the optimal features of STD and FD-NL through correlation and distance correlation.
- The implementation of the bagged Tree-based classifier is developed to mitigate overfitting by introducing randomness and diversity into the ensemble, thereby enhancing its capability to accurately classify epileptic seizures.
- The development of an XAI framework utilizing the SHAP (SHapley Additive exPlanations) model has an explanation behind the reasoning of the proposed model predictions. The visual explanations generated by SHAP facilitate a deeper understanding of the interpretive processes underlying the decisions of the most effective classifiers, as well as identifying the critical features for the detection of epileptic seizures.

The proposed EEG ES detection framework enhances accuracy, mitigates over-fitting issues, and enables optimal feature selection. Tested on the Bonn and UCI-EEG datasets, its versatility and comprehensive approach show promise for streamlining diagnostics process of the patient.

The organization of the paper is as follows: Section 1 and Section 2 present the introduction and related works, respectively. Section 3 show the efficient EEG ES detection framework. Experimental results and discussion are present in Section 5, respectively. Finally, the conclusion of the paper is in Section 6.

2. Related work

This section describes the prior research that used various decomposition methods, linear and non-linear features, optimal feature selection methods, and ML models for efficiently detecting epileptic seizures (ES).

2.1. Wavelet-based statistical and fractal dimension (FD) features extraction with machine learning models

The extraction of essential features from EEG signals are important, especially from different wavelet decomposition levels in EEG epileptic seizure detection. Various studies have been applied wavelet-based features for the accurate classification of pre-ictal, inter-ictal, and ictal states in EEG-based ES detection [11–15].

Recently, Al-Salman et al. [11] applied discrete wavelet transform (DWT) to decompose the brain EEG signals into subbands, further processing to extract diverse wavelet-based features. A Grey Wolf Optimizer (GWO) based deep recurrent neural network (DRNN) was employed to differentiate between seizure and non-seizure signals, achieving 93.4 % accuracy in automatic EEG ES detection. Harendra et al. [16] employed DWT for EEG signal decomposition and extracted statistical features such as standard deviation (std) and mean absolute value (MAV), obtained 90% accuracy. Sharmila et al. [17] applied DWT for EEG signal decomposition and extracted statistical features (STD), average power (AVP), and MAV with KNN and Naive Bayes (NB) classifiers, achieved 97% accuracy . Moreover, R. Uthayakumar et al. [18] introduced six wavelet-based statistical time domain features, such as variance and std, with several ML models, where the Decision Tree (DT) model achieved 97% accuracy. In the last two decades, Fractal Dimension (FD) feature have received much attention, exhibiting satisfactory performance with various feature selection methods and ML [18–20]. A study in [18] introduced an automated system for ES detection using FD theory and the Support Vector Machine (SVM) model reported 90% accuracy. T. M. E. Nijssen et al. [19] implemented various wavelet-based features, such as Higuchi's Fractal Dimension (HFD), Hurst Exponent (HE), and Shannon entropy, in combination with RF and SVM models. Hussain et al. [21] utilized DWT in the preprocessing stage, extracting HFD and Katz Fractal Dimension (KFD) features from DWT subbands and employing SVM for classification. Further, in [22,23], a Cross-Information Potential (CIP) and Tunable-Q Wavelet Transform (TQWT) were examined for EEG signal preprocessing, and the Random Forest (RF) model was used for classification, achieved satisfactory results. A. Nishad et al. [23] employed DWT for decomposition and extracted non-linear features, such as entropy and fractal dimensions and applied a Support Vector Machine (SVM) classifier, where fractal dimensions achieved above 96% overall accuracy. Upadhyay et al. [24] applied the Max Energy to Shannon Entropy ratio to select appropriate EEG channels from each frequency band, calculating three distinct non-linear features and using three machine learning techniques, where Least Square-Support Vector Machine (LS-SVM) showed satisfactory performance. The summary of the various literature shows the importance of STD linear and FD-non linear features with effective ML models in EEG epileptic seizure detectionet al. [25–27].

2.2. Correlation-based feature selection methods with the machine model

Feature selection is an important process that minimizes the number of features utilized by the ML model in EEG epileptic seizure detection [25]. The reduction of the feature set not only simplifies the model's complexity but also facilitates easier interpretation and decreases training time, often leading to enhanced system performance. Correlation, often measured as the relationship between two or more variables, has been widely applied in various fields over the past few decades due to its capability to measure both linear and nonlinear associations between features [13]. Aliyu et al. [14] introduced the

Table 1
Notation table.

Notation	Description
<i>mean</i> _1	Mean feature from decomposition level D3
<i>mean</i> _2	Mean feature from decomposition level D4
<i>mean</i> _3	Mean feature from decomposition level D5
<i>mean</i> _4	Mean feature from decomposition level A5
<i>std</i> _1	Standard deviation feature from decomposition level D3
<i>std</i> _2	Standard deviation feature from decomposition level D4
<i>std</i> _3	Standard deviation feature from decomposition level D5
<i>std</i> _4	Standard deviation feature from decomposition level A5
<i>HFD</i> _1	Nonlinear feature from decomposition level D3
<i>ENT</i> _2	Nonlinear feature from decomposition level D4
<i>PFD</i> _3	Nonlinear feature from decomposition level D5
<i>HFD</i> _4	Standard deviation feature from decomposition level A5

Pearson correlation coefficient (PCC) in the feature selection process, aiming to identify the most pertinent subset of features from the original set. Upon selecting the optimal features via PCC, the model achieved an accuracy of 93.1%. Recently, N.Ji et al. [28] introduced an improved correlation-based feature selection method. The proposed methods select the optimal features from the time, frequency, and entropy features of wavelet decomposition, after which the random forest model performed classification and reported satisfactory performance.

2.3. Motivation

After summarizing the above literature, we are motivated to present a correlation coefficient and distance correlation-based feature selection algorithms, a Bagged Tree-based classifier model with XAI. For the feature selections, we employ p-value analysis to select dominant features, which eliminates the high-correlation features. A Bagged Tree-based classifier is then efficiently applied to differentiate EEG brain signals of seizure and non-seizure EEG states, while the explainable AI interprets and explains the decision-making process of the proposed algorithm automatically without any complex calculation or manual explanation. The next section provides detailed information about the proposed framework for EEG ES detection.

3. Materials and methods

This section presents a novel framework for EEG-based epileptic seizure detection. The framework includes a detailed pipeline for EEG ES detection that presents the EEG data sets, preprocessing, feature extraction, feature selection, and explainable classification steps. Fig. 1 provides the proposed framework for EEG ES detection.

3.1. EEG data collection

Initially, the collected EEG datasets from the UCI and Bonn EEG benchmark datasets are investigated. The Bonn EEG dataset includes non-seizure, transition, and seizure signals [15], while the UCI-EEG dataset consists of non-seizure and seizure signals [16].

3.1.1. Bonn EEG dataset

The Bonn EEG dataset was collected from five patients [15] and categorized into five sets, labeled (A) through (E), each containing 100 single-channel EEG signal collected over 23.6 seconds [18]. The sampling rate of the Bonn EEG data set is 173.61 Hz. Sets A to E involve various EEG states. Specifically, sets (A) and (B) represent different normal EEG signals, with (A) and (B) showing EEG states where the subjects' eyes were open and closed, respectively. Sets C and D presents the transitional states (interictal) between normal and seizure, while set (E) contains EEG readings from five EEG epileptic individuals during seizures. Sets (A) and (B) were obtained non-invasively using the '10-20' international system, and sets (C) and (D) employed invasive

recording methods [18]. Further details of each set within the Bonn EEG dataset are shown in Table 2, and Fig. 2 illustrates EEG epileptic seizures in non-seizure (pre-ictal), transition (Interictal), and seizure (ictal) EEG states. Moreover, the set (CD,E) and (AB,CD,E) are used in the proposed study for segmentation.

3.1.2. UCI-EEG dataset

The UCI-EEG dataset was collected from 5 subjects, each contains 100 file have 4097 data points recorded over 23.5 seconds [27]. Each samples were divided into 23 chunks, representing 1 second of EEG data. After segmentation, chunks were shuffled. The states of the subjects fluctuated between having their eyes open and closed. The target variable 'y', located in column 179, and a binary class y (0,1) including (A,B) set is used for the analysis. It denotes the ictal and pre-ictal states, as detailed in Table 3. In addition, various EEG states of the UCI-EEG dataset are shown in Fig. 3.

3.2. Pre-processing

In this section, the collected EEG signal data passes through a filtering process to eliminate noise and artifacts that could originate from electromyography (EMG), eye blinking, or limb movements during recordings [23,26]. A Butterworth filter is applied on EEG signals within the desired frequency ranges, excluding noise. The Butterworth filter can be mathematically expressed as:

$$H(f) = \frac{1}{\sqrt{1 + \left(\frac{f}{f_c}\right)^{2n}}} \quad (1)$$

$H(f)$ is the frequency response of the filter, f shows the frequency, f_c is the cutoff frequency which is 0.1 Hz, n represents filter order equal to 4. The Nyquist freq is 0.5 Hz. We employ the interpolation-based oversampling method on the each set of the seizur (E) of the Bonn and set B of the UCI EEG dataset to balance.

3.3. Signal splitting

In the preprocessing subsection, we define the optimal segment size for dividing the EEG signal time series into smaller epochs. For the Bonn EEG dataset, we increase the segment size using the optimal values of epoch = 0.5 and epoch_step = 0.023 as shown in Table 2, while the UCI EEG dataset have no segmentation process.

Algorithm 1 Signals Splitting

```

1: Load the EEG signal  $t$  time series data,  $k = 0$ 
2: Window  $w_{size}$ , window  $w_{over}$ 
3: while  $k > 0$  do
4:   Select window size  $w_{size}$  and overlap  $w_{over}$ 
5:   Calculate the performance of  $w_{size}$  and  $w_{over}$ 
6:    $k++$ 
7:   Calculated the performance of the feature vector
8: end while

```

3.4. Signals decomposition and feature extraction

This subsection emphasizes the decomposition of the EEG signals and critical feature extraction from the EEG signals. The proposed feature extraction methods are explained in Algorithm 2 and have two primary steps: (1) EEG signal decomposition and (2) feature extraction. The non-stationary nature of EEG time-series signals, which contain high-frequency data and other important information, as well as large frequency oscillations, employing solely the fast Fourier transform (FFT) for signal analysis, proves insufficient due to its limitation to extracting merely the frequency information of time-series signals [17]. The wavelet transform method of multi-resolution decompose signals into various frequency bands and represents a time function

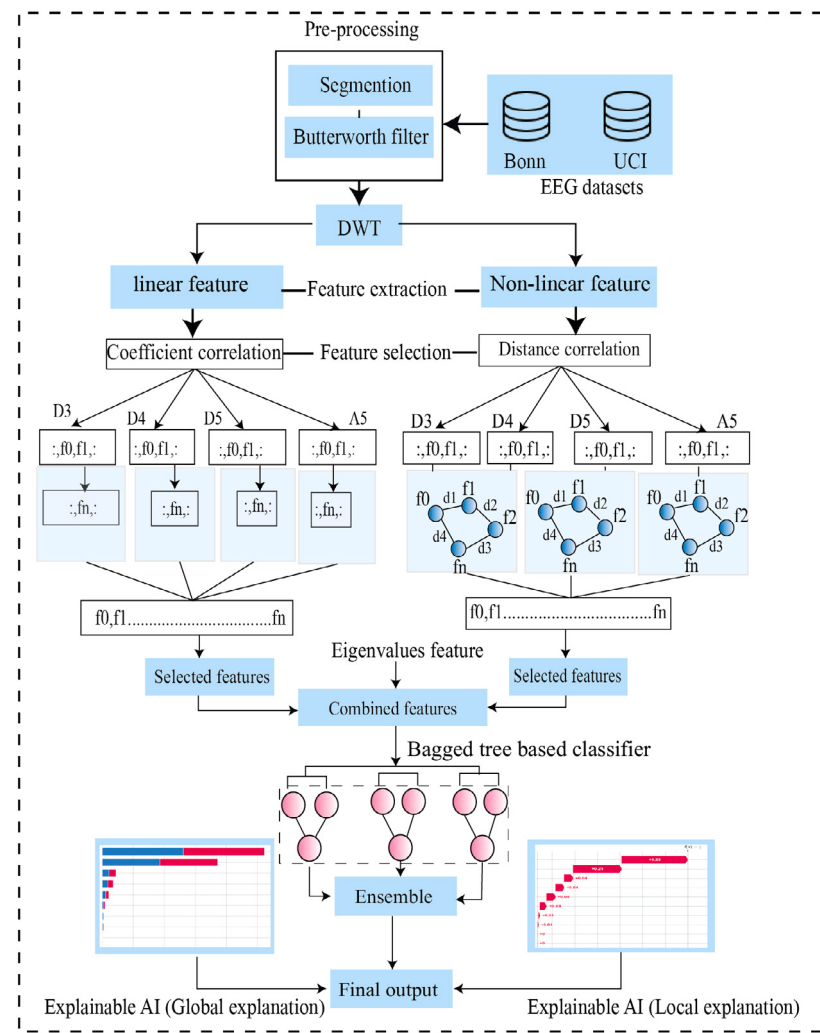


Fig. 1. The block diagram of the proposed framework for EEG epileptic seizure detection.

Table 2

The detailed description of the Bonn EEG segments dataset.

Classification set	Stages	Segments, sample	Number of files
(A)	Patient eyes opened (Pre-ictal)	(8600,1338)	100
(B)	Patient eyes closed (Pre-ictal)	(8600,1338)	100
(C)	Inter-ictal	(8600,1338)	100
(D)	Inter-ictal	(8600,1338)	100
(E)	Ictal	(8600,1338)	100

Table 3

Full description of the UCI-EEG dataset.

Classification set	Stages	Sample length	Number of files
(A)	Ictal	2300	100
(B)	Tumour region (Pre-ictal)	2300	100
(C)	Healthy region (Pre-ictal)	2300	100
(D)	Healthy region (Pre-ictal)	2300	100
(E)	Healthy region (Pre-ictal)	2300	100

using fundamental units called wavelets. One significant advantage of wavelet transforms is their ability to adapt the window size, enabling them to narrow for low frequencies and widen for high frequencies. This adaptability results in superior time-frequency resolution across different frequency bands. EEG signals, which contain a rich set of features, can be effectively compressed into a reduced set of features through spectral analysis and the extraction of high-frequency data. The continuous wavelet transform and discrete wavelet transform are

mathematically represented as follows:

$$CWT_{(c,d)} = \int_{-\infty}^{\infty} y_t \psi_{c,d} * y(y) dy \quad (2)$$

where y_t presents the EEG signal under analysis, and c represents the compression coefficient with dilation, translation, and scaling relevant to the time axis. The asterisk superscript denotes complex conjugation.

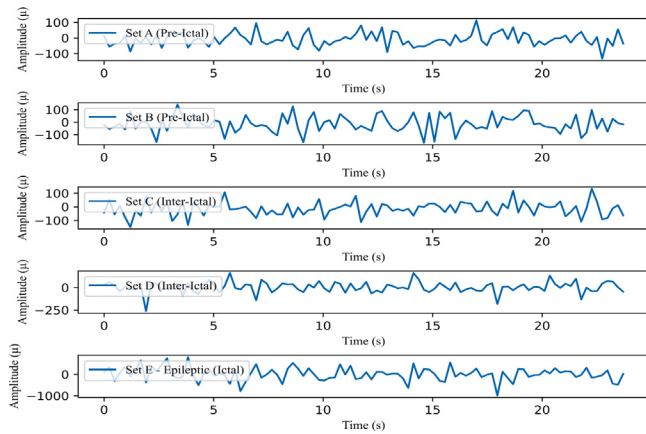


Fig. 2. Various types of EEG signals in the Bonn EEG dataset (interictal, pre-ictal, and ictal).The x-axis shows the time samples of EEG signal and y-axis shows the amplitude include different EEG states of the subjects.

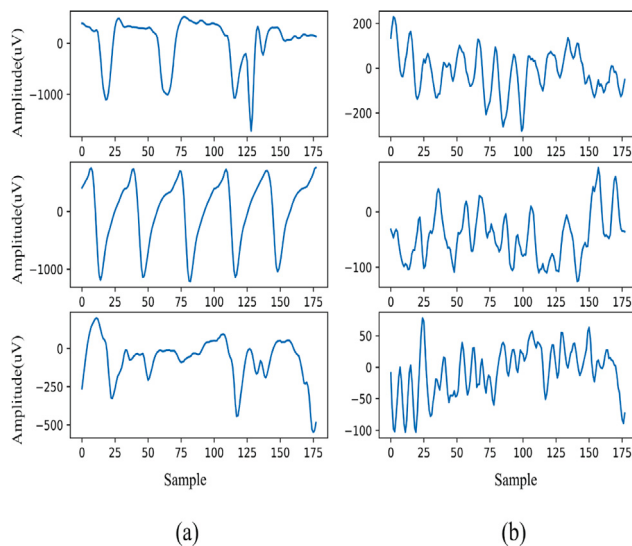


Fig. 3. EEG signals in the UCI-EEG dataset. The x-axis shows the samples of EEG signal and y-axis shows the amplitude. (a) shows the ictal signals of the different subjects have high amplitude and variation , (b) present the pre-ictal signals have normal EEG state of the subjects.

Additionally, $\psi_{c,d}$ is computed as the wavelet over time and scale:

$$\psi_{c,d}(t) = \frac{1}{\sqrt{|c|}}\psi\left(\frac{t-d}{c}\right) \quad (3)$$

Where $\psi_{c,d}(t)$ shows the wavelet and CWT translation and scaling parameters can be changed continuously. However, determining wavelet coefficients for every possible scale can be computationally intensive and produce considerable data, thus often positioning DWT as a preferred alternative method. The wavelet transform is an extension of the conventional Fourier transform.

In DWT, initially the input EEG signals $x[n]$ are segmented into low-pass $g[n]$ and high-pass $h[n]$ filters. The output from these filters is represented by coefficient $D1$ and approximation $A1$, respectively. Symbols D_n and A_n denote the frequencies of the input EEG signals. The decomposition process is iteratively performed to acquire subsequent coefficient levels, with a five-level decomposition being executed in this study. Each step of decomposition enhances frequency resolution while down-sampling diminishes time resolution, as illustrated in Fig. 4.

The same procedure is applied to the UCI-EEG dataset using the Daubechies 1 (db1) wavelet. Each decomposition level captures the

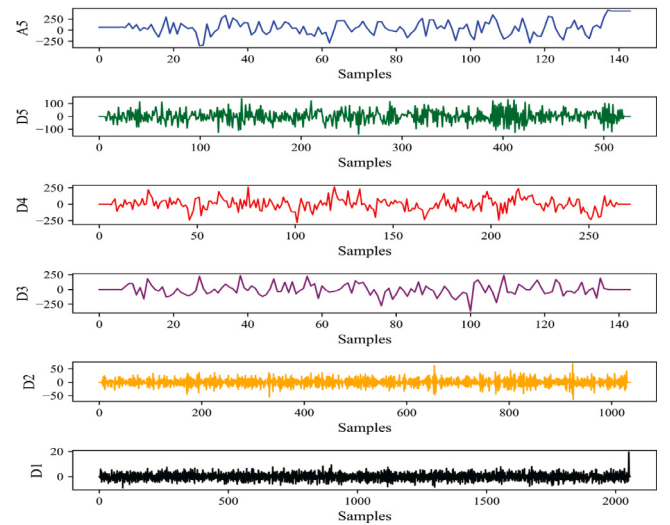


Fig. 4. The decomposition level of Bonn EEG dataset using DWT. The x-axis shows the samples of EEG signal and y-axis present the amplitude. From D1 to D5 shows various decomposition level have different frequency.

Table 4

Decomposition levels of Bonn and UCI EEG dataset existing various frequencies (Hz).

Sub-band	Frequency (Hz)	Decomposition level
Detail D5	[3–6]	5
Detail D4	[6–12]	4
Detail D3	[12–25]	3
Detail D2	[25–50]	2
Detail D1	[50–100]	1

important frequency components essential for seizure detection in EEG signals as shown in Table 4.

For epilepsy detection, the frequency range is typically from 2 to 30 Hz. As a result, the coefficients $D1, D2$ are removed from processing due to their high-frequency range. Thus, the approximation coefficients ($D3; D4; D5, A5$) of each channel are considered. Each subband encompasses 12 FD-based nonlinear and 8 statistical features from both the Bonn and UCI-EEG datasets in proposed study.

3.5. Feature extraction methods

This subsection describe the feature extraction process from each subband, including different FD-based non-linear (FD-NL) and statistical time domain (STD) features [21]. These features are important for describing the characteristics of the EEG signals and enabling differentiation between various EEG states. FD-nonlinear features, extracted from the EEG signal's show the complexity and irregularity of the EEG signals [21]. Moreover, statistical time-domain features present the amplitude and distribution of the signal by encapsulating its statistical properties [17]. In the proposed study two STD features consist of mean, standard deviation (std) are extracted from each subband of the approximation coefficients. Therefore, a total of 8 features are extracted . The mathematical expressions for the STD features in this study are given below.

$$\text{Mean} = \frac{1}{X} \sum_{i=1}^X x_i \quad (4)$$

where X is the total number of values, and x_i are the individual data points.

$$\text{Std} = \sqrt{\frac{1}{X-1} \sum_{i=1}^X (x_i - \text{Mean})^2} \quad (5)$$

Algorithm 2 Feature Extraction Methods

```

function SIGNAL( $E_s, k0, F_S, D_L, w_{size}, over_{size}$ )
2:   Load  $E_s$  and initialize epoch  $k = 0$ 
   Initialize feature vector  $FV$  as an empty list
4:   for each  $w_{size}$  and  $w_{over}$  do
   while  $k \geq 0$  do
6:     for each signal  $S$  in  $E_s$  and level  $L$  in  $D_L$  do
       Decompose  $S$  using WT at level  $L$ 
8:       Extract FD-Nonlinear features
       Extract Statistical time domain (STD) features
10:      end for
       Append feature vector to  $FV$ 
12:      Evaluate performance using various Feature Metrics (FM)
       Increment epoch:  $k++$ 
14:    end while
       Apply dimensional reduction to  $FV$ 
16:  end for
   return distinguishable feature vector  $FV$  of EEG signals
18: end function

```

The features extracted from each subband encompass several measures, including Detrended Fluctuation Analysis (DFA), Shannon Entropy (SE) and Higuchi Fractal Dimension (HFD). The detailed explanations and mathematical computing of the fractal dimensions and entropy-based measures can be found in existing literature [17,18]. The FD-NL features are as follows:

$$SE = - \sum_{i=1}^N P(x_i) \log_2 P(x_i) \quad (6)$$

where $P(x_i)$ is the probability of a given value x_i occurring in the time series.

$$HFD = \frac{\log_{10}(L(k))}{\log_{10}(1/k)} \quad (7)$$

where $L(k)$ is the length of the time series for a given k and the slope is estimated over a range of k values.

To compute DFA the integrated time series $Y(k)$ from the original time series $X(i)$, where $i = 1, 2$.

$$Y(k) = \sum_{i=1}^k [X(i) - X_{avg}] \quad (8)$$

where X_{avg} is the average of $X(i)$. After, divide $Y(k)$ into N non-overlapping intervals of equal length n . In each interval v , fit $Y_v(k)$ (in the interval) with a least squares line fit $v(k)$. The v represents the v th interval. The fluctuation $F(n)$ is then computed by averaging the residuals from all intervals and then taking the square root:

$$F(n) = \sqrt{\frac{1}{N} \sum_{v=1}^N \sum_{k=1}^n [Y((v-1)n+k) - Y_v(k)]^2} \quad (9)$$

The procedure is repeated for all time scales (window sizes) n to provide a relationship between $F(n)$ and the window size n . The fluctuations can be related to the size of the window by a power law:

$$F(n) \propto n^H \quad (10)$$

After extracting features from the selected decomposition level are passed feature selection methods are discussed in the next section.

3.6. Feature selection methods

3.6.1. Correlation Coefficient Analysis (CCA)

To present the relationships between variables, we applied Pearson correlation (PC), which yields values ranging between -1 (indicating

a strong negative relationship) and 1 (indicating a strong positive relationship). The feature data consists of n paired data points, and the PC, denoted as r_{xy} given below:

$$r_{xy} = \frac{\sum_{i=1}^n (x_i - \bar{x})(y_i - \bar{y})}{\sqrt{\sum_{i=1}^n (x_i - \bar{x})^2 \sum_{i=1}^n (y_i - \bar{y})^2}} \quad (11)$$

The x_i and y_i represent individual sample points with index i , while \bar{x} and \bar{y} denote the means of variables x and y respectively, and n symbolizes the total number of data points, the summation symbol $\sum_{i=1}^n$ signifies the sum over all n data points. In addition, several experiments are conducted to find the optimal Correlation Coefficient (CC) is 0.8. Features exhibiting correlation above this CC threshold are excluded. The comprehensive overview of mathematical computing of the correlation coefficient is shown in Algorithm 3.

Algorithm 3 Feature selection via Correlation Coefficient

```

1: function CORRELATION, B_ELIMINATION(Data matrix  $X$ , Target vector  $y$ ,
   Significance level  $\alpha$ )
2:   Compute the correlation matrix  $C$  of  $X$ 
3:   for each pair of features  $(i, j)$  do
4:     if  $C_{i,j} = 0.82$  then
5:       Remove one feature from the pair
6:     end if
7:   end for
8:   Define the initial feature subset as NULL
9:   while not all features  $f$  are evaluated do
10:    Compute  $p$ -values for remaining features  $f$  relative to target
     $y$ 
11:    for each feature  $f$  do
12:      if  $p$ -value of  $f < \alpha$  then
13:        Remove feature  $f$ 
14:      end if
15:    end for
16:     $f \leftarrow$  Remaining features
17:  end while
18: end function

```

Fig. 6 shows the distribution of the selected features after first elimination. In the next elimination process, the STD features are selected for various cases and datasets. In the case (CD,E) from the Bonn EEG dataset, five STD features were chosen mean_3,mean_4, mean_2, mean_1, and std_1. Similarly, in the case (AB, CD, E), six STD features are selected: mean_4,mean_3, mean_2, mean_1, std_1, and std_2. Finally, in the case (A, B) from the UCI-EEG dataset, six STD features are selected: mean_3, mean_2, mean_1,mean_4 std_1 and std_2 as shown in Fig. 5. The explanation of the eigenvalue features and their respective decomposition levels is presented in Table 1.

3.6.2. Distance correlation

The distance correlation is utilized to manage the variability of feature values, predominantly for nonlinear features. The distance correlation analysis applied in the proposed study includes four steps as follows.

A) Compute Pairwise Distances

Let $U = \{u_1, u_2, \dots, u_n\}$ and $V = \{v_1, v_2, \dots, v_n\}$ represent the data sets for two random variables at each decomposition level feature. First, the pairwise distance matrices, M and N for U and V , respectively, are computed. For a one-dimensional data set, the absolute difference between the elements is given below:

$$M_{ij} = |u_i - u_j|, N_{ij} = |v_i - v_j| \quad (12)$$

B) Compute double-centered distance matrices

The double-centered distance matrices, M^* and N^* , are derived from M and N respectively as follows:

$$M_{ij}^* = M_{ij} - \frac{1}{n} \sum_{k=1}^n M_{ik} - \frac{1}{n} \sum_{k=1}^n M_{kj} + \frac{1}{n^2} \sum_{k=1}^n \sum_{l=1}^n M_{kl}, \quad (13)$$

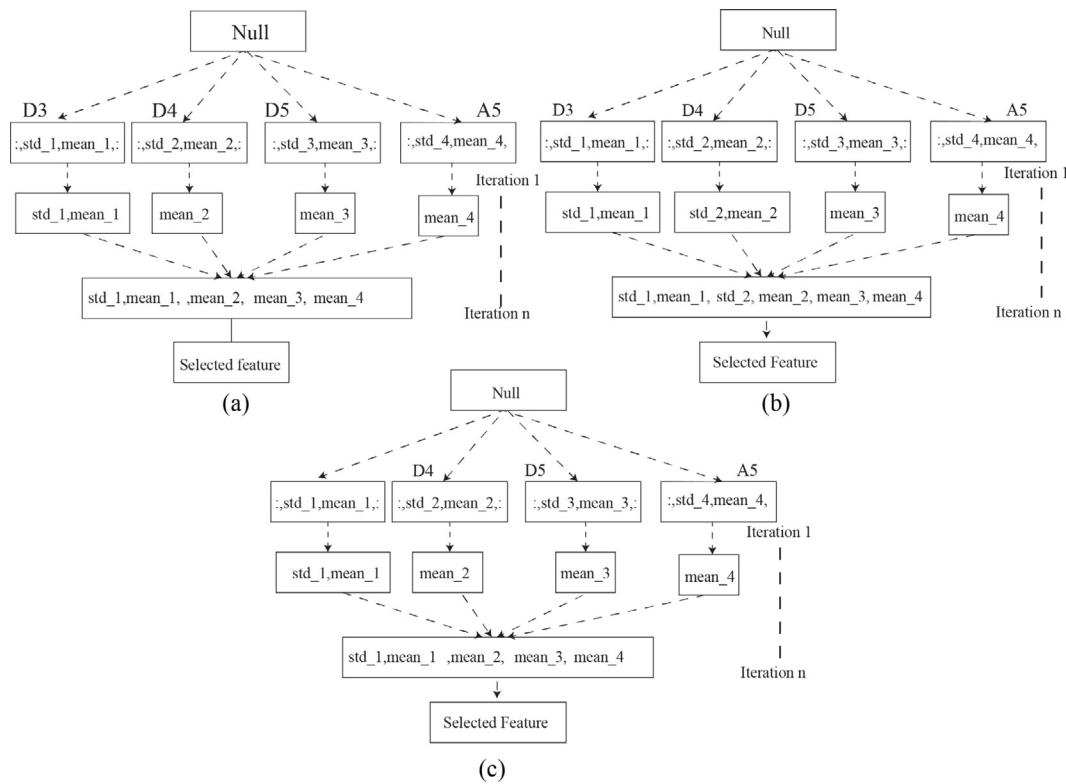


Fig. 5. The block diagram of coefficient correlation. (a),(b) the extracted eigenvalue feature set of the Bonn EEG dataset, (c) the UCI-EEG dataset.

$$N_{ij}^* = N_{ij} - \frac{1}{n} \sum_{k=1}^n N_{ik} - \frac{1}{n} \sum_{k=1}^n N_{kj} + \frac{1}{n^2} \sum_{k=1}^n \sum_{l=1}^n N_{kl} \quad (14)$$

where M_{ij} and N_{ij} represent the pairwise distances and n indicates the total number of observations. C) Calculate distance variances

The distance variance, $V(U, U)$, for a variable U is computed as follows:

$$V(U, U) = \frac{1}{n^2} \sum_{i=1}^n \sum_{j=1}^n (M_{ij}^*)^2 \quad (15)$$

Similarly, the distance variance, $V(V, V)$, for V is:

$$V(V, V) = \frac{1}{n^2} \sum_{i=1}^n \sum_{j=1}^n (N_{ij}^*)^2 \quad (16)$$

D) Calculate distance correlation

The distance correlation, $R(U, V)$, is calculated as the square root of the distance covariance normalized by the square root of the product of the distance variances:

$$R(U, V) = \sqrt{\frac{V(U, V)}{\sqrt{V(U, U)V(V, V)}}} \quad (17)$$

The values of $R(U, V)$ range between 0 and 1, with 0 signifying complete independence between variables, and 1 indicating perfect dependence. Various distance correlation values are used to identify highly correlated features, and performance was assessed post-elimination, employing an optimal distance correlation value of 0.7 for elimination.

Fig. 6 shows the distribution of the selected features after elimination.

After the elimination process, eight FD-NL features (HFD_1, ENT_1, ENT_2, HFD_2,HFD_4, PFD_1,PFD_2, PFD_3) from the case (CD,E) and six D-NL features (HFD_1, ENT_1, PFD_1,PFD_2, PFD_3, HFD_4) feature are selected in the (AB,CD,E) set case of Bonn EEG dataset ,while the same number of features from the case (A, B) of the UCI-EEG dataset.

Fig. 7 illustrates the comprehensive process of distance correlation while the descriptions and decomposition levels of the selected features are shown in **Table 1**.

3.7. Classification model

3.7.1. Bagged tree-based classifier (BTBC)

In this subsection, the proposed model is explained in detail. The Bonn and the UCI-EEG datasets are highly imbalanced and consist of fewer seizure or ictal samples than non-seizure or preictal instances. So, therefore, the imbalanced feature data created has the potential to bias the model towards over-fitting [5,26,28,29]. To address this issue, we employ a bagging technique with a decision tree in the proposed study. A Bagged Tree-based classifier model implements the bagging mechanism to efficiently differentiate different EEG states, especially the inter-class variation [30] and is distinct from a conventional random forest model. Moreover, the bagging mechanism utilizes different individual decision trees to independently classify each feature data bootstrap and then aggregates the outcomes through a voting process to determine the final result, as detailed in Algorithm 4.

Algorithm 4 Bagging Tree-based Classifier

```

1: Input: EEG dataset  $D$ , number of bootstrap samples  $B$ , base classifier  $C$ 
2: Output: Tree-based classifier  $E$ 
3: for  $b \leftarrow 1$  to  $B$  do
4:   Sample  $D_b$  from  $D$  with replacement
5:   Train base classifier  $C_b$  on  $D_b$ 
6: end for
7: function ENSEMBLEPREDICT( $x$ )
8:    $votes \leftarrow \{0, 0, \dots, 0\}$ 
9:   for  $b \leftarrow 1$  to  $B$  do
10:     $c \leftarrow PREDICT(C_b, x)$ 
11:     $votes[c] \leftarrow votes[c] + 1$ 
12: end for
13: return ARGMAX( $votes$ )

```

The proposed model has three main steps to perform the classification process;

Step 1: Input feature data

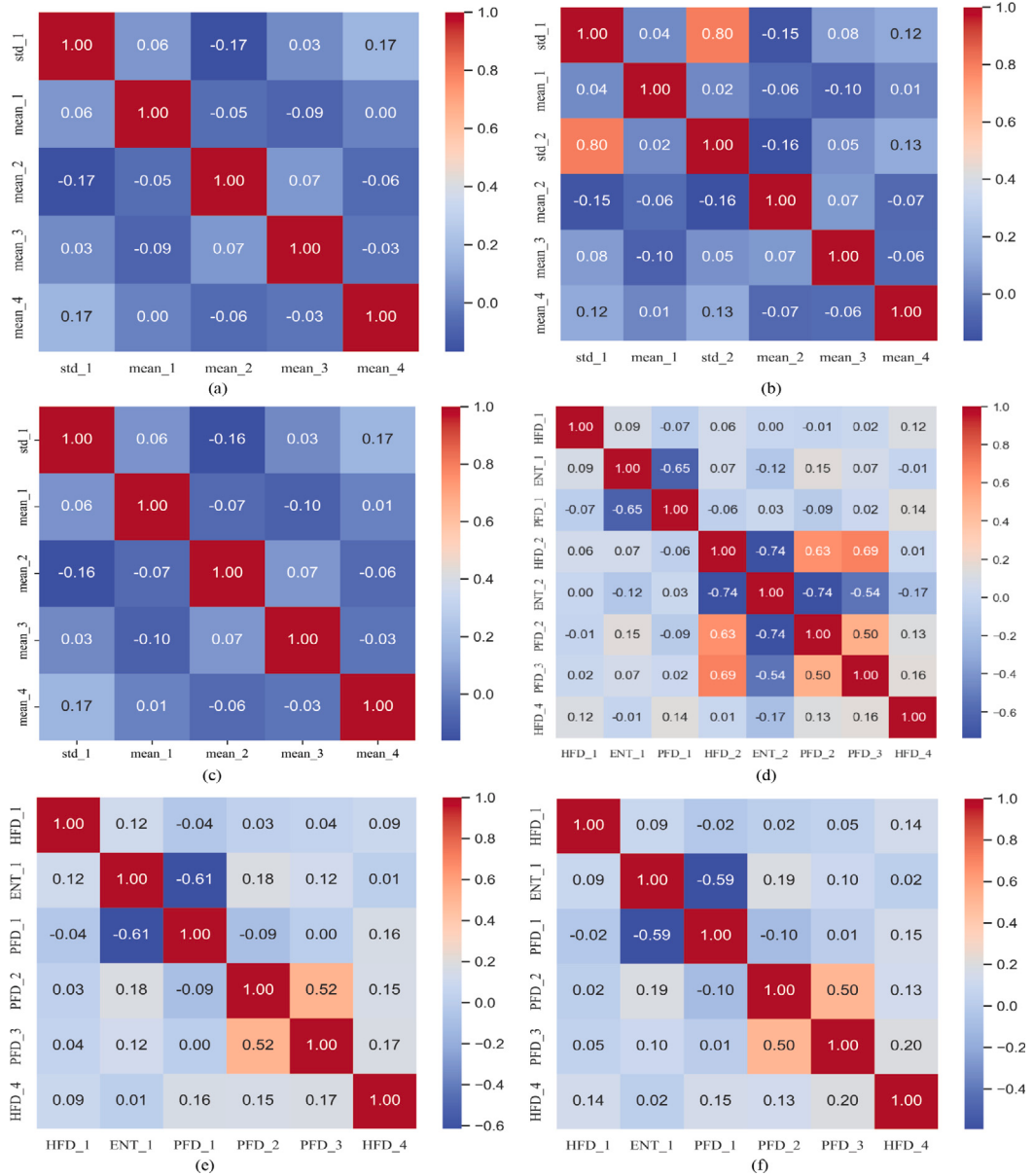


Fig. 6. The Correlation coefficient and distance correlation matrix after elimination of highly correlated features. (a),(b),(d),(e) STD linear and FD-based non-linear eigenvalue feature selected after second elimination using Bonn EEG dataset ,(c),(f) for UCI- EEG dataset.

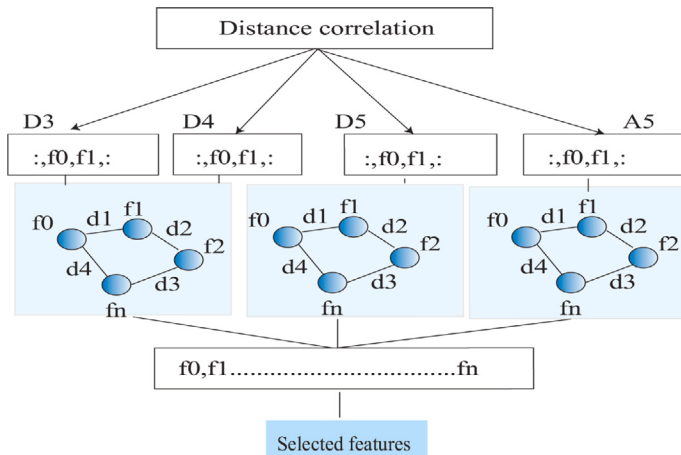


Fig. 7. The block diagram of distance correlation include different decomposition level and distance correlation between feature set .

Table 5

The hyper-parameters for the proposed model in EEG ES detection.

Model	Hyperparameter search space
Proposed model	<code>n_estimators = 100, max_features = sqrt, max_depth = 1, min_samples_split = 5, min_samples_leaf = 10, bootstrap = True, random_state = 42</code>

The proposed BTBC takes the input feature data represented as D . The EEG dataset encompasses various STD linear and Fractal Dimension (FD) based nonlinear features. The model also requires the number of bootstrap samples B and employs a decision tree as the base classifier C .

Step 2: Bootstrap sampling and model training

In the bootstraps of the proposed model, for each of the B bootstrap samples, a distinct subset D_b is derived from D , with variable sample sizes promoting diversity among samples. This subset is selected with replacement, allowing some instances to repeat, while others may be excluded. Each decision tree C_b is trained on its respective D_b , focusing on optimal splits that minimize the target variable's heterogeneity in the child nodes. The training process continues until it meets a predefined stopping criterion. The process of this step is a collection of B decision trees, each adapted to a uniquely composed feature data set, as shown in [Table 5](#).

Step 3: Prediction function

The function `EnsemblePredict(x)` in the proposed model is designed for making predictions on new data points x . This function operates by initializing an array of `votes` for storing class votes. Each tree C_b in the ensemble contributes to the prediction for x , with its vote being weighted based on its accuracy, refining the traditional majority voting mechanism. The class accumulating the highest weighted vote count is then selected as the prediction for x . The proposed model, with its emphasis on customized bagging and weighted voting, offers advantages such as enhanced handling of high-dimensional data, improved robustness against overfitting, and the ability to model complex, nonlinear relationships. Additionally, it provides valuable insights into feature importance, aiding in identifying key predictors for seizure occurrences in EEG data.

4. Explainable Artificial Intelligence (XAI)

In this section, we discuss the interoperability of the proposed model. XAI helps by offering insights into the AI model's decision-making process. It allows medical experts to validate the model's predictions and make more informed and reliable decisions regarding patient diagnosis and treatment [9,10]. Moreover, it makes the decision more understandable so that even non-experts or family members of the patients can easily understand the decision, as shown in [Fig. 1](#). Recent studies in machine learning (ML) for biomedical signal analysis highlight the urgent need to make their outputs comprehensible [9]. This has led to the rise of XAI systems in smart healthcare systems [10]. Although ML models tend to be more interpretable than deep learning models because of their explainable structure, achieving full interpretability in decision tree classifiers remains a challenge. The proposed model employs SHapley additive exPlanation (SHAP) model of XAI to elucidate its decision-making processes, feature importance, and inherent biases. Some of the recent XAI methods from the literature [9,10] are detailed below:

(A) Text Explanations: The method compute a relevance score for the variables utilized by the model, thereby furnishing an intricate understanding of the model internal process of decision making.

(B) Local Explanations: This involves understanding the model's responses to minor input changes.

(C) Representative Explanations: Assesses how training data influences the decision-making process.

(D) Visual Explanations: The specific decision trees that inform outcomes.

5. Experimental results

This section provides the experimental setup, presents an empirical analysis of the experimental results, and provides an interpretation and explanation of the proposed model's classification performance.

5.1. Experimental setup and performance metrics

The proposed framework has been experimentally executed using a system configure with a central processing unit (CPU), an NVIDIA Jetson Nano Developer Kit GPU, and a Windows 10 (64-bit) operating system. The system utilizes Python 3.7 within a notebook environment, incorporating libraries such as TensorFlow, PyEEG, Pandas, Keras, NumPy, and Scikit-Learn. The experiments is conducted on the Bonn and UCI EEG datasets [17,27]. Various machine learning models, including RF, LR, DT, XGB, and NB are employed with the proposed model in EEG epileptic seizure (ES) detection. The configuration and execution settings for the proposed model were constant across all experimental types having parameters shown in [Table 5](#).

In this study, two significant cases from the Bonn EEG dataset are used for binary and multi-classification problems related to EEG ES detection: sets (CD, E) and (AB, CD, E). In these sets, E represents *seizure*, while AB is categorized as *non-seizure*. In the analysis of the UCI-EEG dataset, a single experimental case (A, B) is considered to differentiate between *seizure* and *non-seizure*. The proposed study used 5-fold cross-validation as a data selection method. In order to address the limitations of a small dataset, data segmentation is performed. Moreover, the classification performance of each ML model is evaluated using various performance metrics, such as accuracy (ACC), precision (PR), sensitivity (SE), specificity (SP), and the F1-score [25,26].

$$ACC(\%) = \frac{T_{Positive} + T_{Negative}}{N} \quad (18)$$

Where, $N = T_{Positive} + T_{Negative} + F_{Positive} + F_{Negative}$

$$PR(\%) = \frac{T_{Positive}}{T_{Positive} + F_{Positive}} \quad (19)$$

$$RE(\%) = \frac{T_{Positive}}{T_{Positive} + F_{Negative}} \quad (20)$$

$$SP(\%) = \frac{T_{Negative}}{T_{Negative} + F_{Positive}} \quad (21)$$

$$F1 = 2 * \frac{RE * PR}{RE + PR} \quad (22)$$

where True Positive (TP), True Positive (TN), False Positive (FP), and False Negative (FN) denote the total number of correctly detected positives (seizure), correctly detected negatives (non-seizure), incorrectly predict positives, and incorrectly predict negatives, respectively.

5.2. The time complexity of the feature extraction methods

In the process of feature extraction, different wavelet features, as mentioned in subsection [Section 3.5](#) are extracted from DWT subbands. Moreover, the execution time of the feature plays an important role in rule-based hardware implementation. The study also examines the feature extraction time of the best eigenvalue feature individually in the experiment. [Fig. 8](#) shows the execution time of the features. The execution times are repeated in different experimental cases, therefore, we select the average of the time complexities. All the features have less time complexity as compared to the relevant literature [16–18].

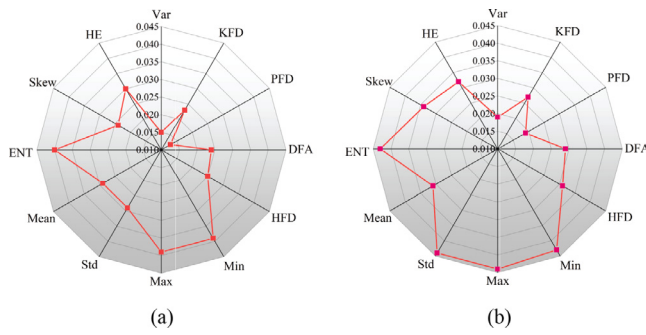


Fig. 8. The execution time of the eigenvalue feature. (a) shows the experiment type of Bonn EEG dataset, (b) UCI-EEG dataset. The value from the origin represents the execution time (sec).

5.3. Analysis and performance of different coefficient and distance correlation measure

This subsection empirically evaluates the optimal features mentioned in subsections Section 3.6.1 and Section 3.6.2. The approach uses two experimental types from the Bonn EEG dataset and one from the UCI-EEG dataset, with varying correlation coefficient (CC) values (0.5, 0.6, 0.7, 0.8, and 0.9) to determine their respective accuracies(%).

Fig. 9 (a) illustrates that accuracy increases when the CC value reaches 0.8. Beyond the 0.8 threshold value, the average accuracy across experiments is constant. Specifically, at CC = 0.8 or greater, the experimental type (CD, E) from the Bonn EEG dataset, utilizing features provided in subsection Section 3.6.1 shows a maximum accuracy of 99.50%. Similarly, the case (AB, CD, E), incorporating features mentioned in subsection Section 3.6.1, reports an equivalent accuracy.

In Fig. 9 (b), a similar performance is observed up to CC = 0.9 for the UCI-EEG dataset. Across all experiments involving different CC values. Moreover, the proposed selected feature of the STD from experimental type (A, B) yielded the highest accuracy up to 98% in EEG epileptic seizure detection.

Fig. 9 (c),(d) depicts the performance for non-linear feature selection from wavelet decomposition using distance correlation (DC). The accuracy increases until DC = 0.7, subsequently stabilizing. At DC = 0.8 and DC = 0.9, the optimal non-linear features from subsection Section 3.6.2, applied to the experimental type (AB, CD, E), achieve a maximum accuracy of 99.5%. For the experimental type (CD, E), features selected from subsection Section 3.6.2 reported an accuracy of 99.50%. A parallel process is observed for the UCI-EEG dataset, where features from subsection Section 3.6.2 at DC = 0.7 from the experimental type (A,B), show a maximum accuracy of 99.60%.

5.4. Ablation study

This subsection presents the training and testing performance of the proposed model. The over-fitting of the model is illustrated through training vs testing accuracy and training loss vs testing loss with respect to the number of trees, as shown in Fig. 10, with effective learning from the optimal linear and non-linear features, the model achieved a training accuracy of 99.5% and a loss of 0.001%, whereas the maximum validation accuracy reached 99.40% with a loss of 0.001% after employing 50 trees. As the number of trees increases, the model progressively enhances the accuracy and reduces the loss to 0.001%, due to the bagged tree approach handling the over-fitting issue efficiently. After the number of trees increases, it has no effect on the model's performance. The same process is repeated for the loss of the proposed model using the experimental type of both types Bonn and UCI EEG datasets.

Table 6
The computational time of the proposed framework in EEG ES detection.

n Procedure	Time (sec)
Pre-processing	4
Feature extraction	10.40
Feature selection	14.10
Classification	10.03

5.5. Experimental analysis and performance of the proposed model

In this subsection, we discuss the comprehensive results of the proposed model. Initially, the Receiver Operating Characteristic (ROC) curve is utilized to evaluate the model's efficiency, as shown in Fig. 13 which presents the ROC curve of the proposed classifier, derived from various EEG class detection systems. For the ROC we used the extra experimental case (C,E) to check the performance of the proposed model on single set. The proposed model achieved averages of 0.99 and 1.00, respectively. Moreover, we also discuss the extended indicators of performance, including the False Detection Rate (FDR), False Omission Rate (FOR), False Positive Rate (FPR), and False Negative Rate (FNR). Furthermore, Fig. 12 shows the superior performance of the proposed model, achieved average rates of FDR (0.029), FPR (0.025), FOR (0.03), and FNR (0.028) for both experimental type of the UCI-EEG dataset. In on experimental type of the Bonn EEG dataset, the model demonstrates the FDR of 0.024, FPR of 0.02, FOR of 0.025, and FNR of 0.023 in EEG epileptic seizure detection.

Additionally, Table 6 presents the average computation time for each experimental type, which shows the proposed model is time efficient.

5.6. Comparison with baseline approaches

The empirical analysis of the proposed model is conducted and compared with some baseline approaches, such as the LR, XGB, DT, NB, and RF using optimal linear and non-linear features. Fig. 11 shows each model's mean accuracy using 5-fold cross-validation. In Fig. 11(a) and (b) highlight that the proposed model employing optimal features, achieved the highest mean accuracy. For the Bonn EEG dataset, mean accuracies are 99.50% and 99.50% for the experimental type (CD,E) and (AB, CD, E) respectively, in EEG ES detection, while XGB reported the lowest mean accuracy. Furthermore, Fig. 11 (c) indicates the proposed model achieved the highest mean accuracy, 99.60% for the (A, B) experiment type of the UCI EEG dataset , with the LR model yielding the lowest performance.

Moreover, Table 7 and Table 8 present the extended performance of the proposed model with other ML classifiers. The proposed model uses optimal features, and achieved the best performance using the experimental type (CD, E) from the Bonn EEG dataset, having a mean accuracy of 99.50%, precision of 99.42%, sensitivity of 99.40%, specificity of 99.42%, and F1-score 98.40%. Moreover, in the case (AB, CD, E) of the Bonn EEG data set the proposed model achieved 99.50% accuracy, 99.40% precision, 99.30% sensitivity, 99.42% specificity, and 99.20% F1-score. For the experimental type of (A, B) of the UCI-EEG, the model reported 99.60% accuracy, 99.50% precision, 99.40% sensitivity, 99.40% specificity, and 99.30% F1-score , the proposed classifier outperformed other machine learning models achieved the best performance on all experimental type of both EEG data. On the other hand, the LR and XGB had the lowest performance among all the models.

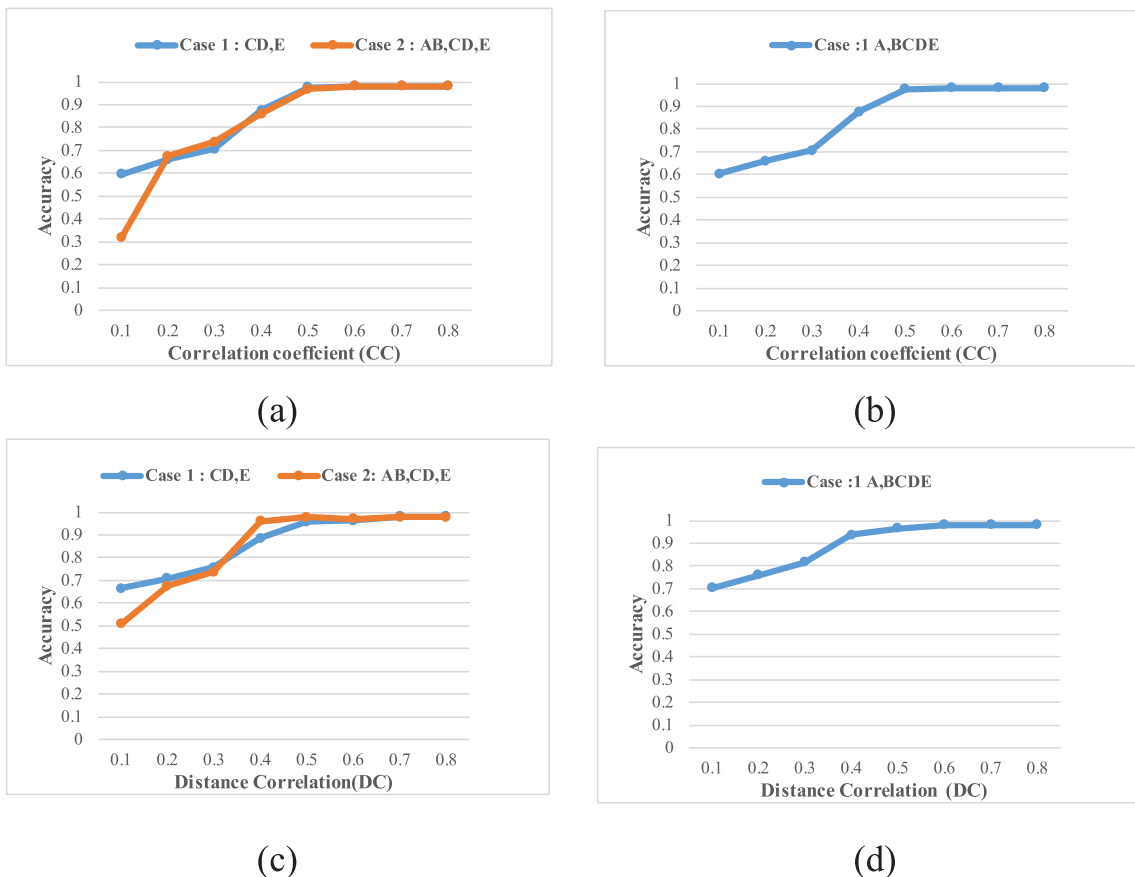


Fig. 9. Correlation coefficient (CC) and distance correlation (DC) based accuracy. (a) shows the impact of the CC and DC threshold value on the performance of the proposed model using Bonn EEG dataset, (b),(d) UCI-EEG dataset.

Table 7

The experimental results of the proposed model with other sibling ML models using 5-fold cross-validation of the experiment type of Bonn EEG dataset.

Methods	Experiment type	Mean			
		ACC (%)	PR(%)	RE(%)	SP(%)
DT	(CD,E)	95.49	95.10	94.50	94.10
	(AB,CD,E)	94.90	92.40	94.90	91.40
XGB	(CD, E)	95.49	94.50	94.43	94.10
	(AB,CD,E)	92.80	92.80	92.60	92.50
RF	(CD,E)	97.10	96.50	96.50	96.40
	(AB,CD,E)	97.10	97.10	97.00	97.70
NB	(CD,E)	93.40	93.80	93.80	93.70
	(AB,CD,E)	93.20	92.80	92.20	92.10
LR	(CD,E)	93.07	92.20	92.10	92.05
	(AB,CD,E)	93.60	93.30	93.20	92.90
Proposed model	(CD,E)	99.50	99.42	99.40	99.42
	(AB,CD,E)	99.50	99.40	99.30	99.40

Table 8

Experimental results of the proposed model using 5-fold cross-validation of the experiment type of UCI EEG dataset.

Methods	Experiment type	Mean			
		ACC (%)	PR(%)	RE(%)	SP(%)
RF	(A,B)	97.90	97.05	97.00	96.80
XGB	(A,B)	97.80	96.59	96.10	96.00
DT	(A,B)	97.90	97.80	97.00	96.90
NB	(A,B)	94.40	94.10	93.00	93.90
LR	(A,B)	94.43	93.40	93.40	93.10
Proposed model	(A,B)	99.60	99.50	99.40	99.40

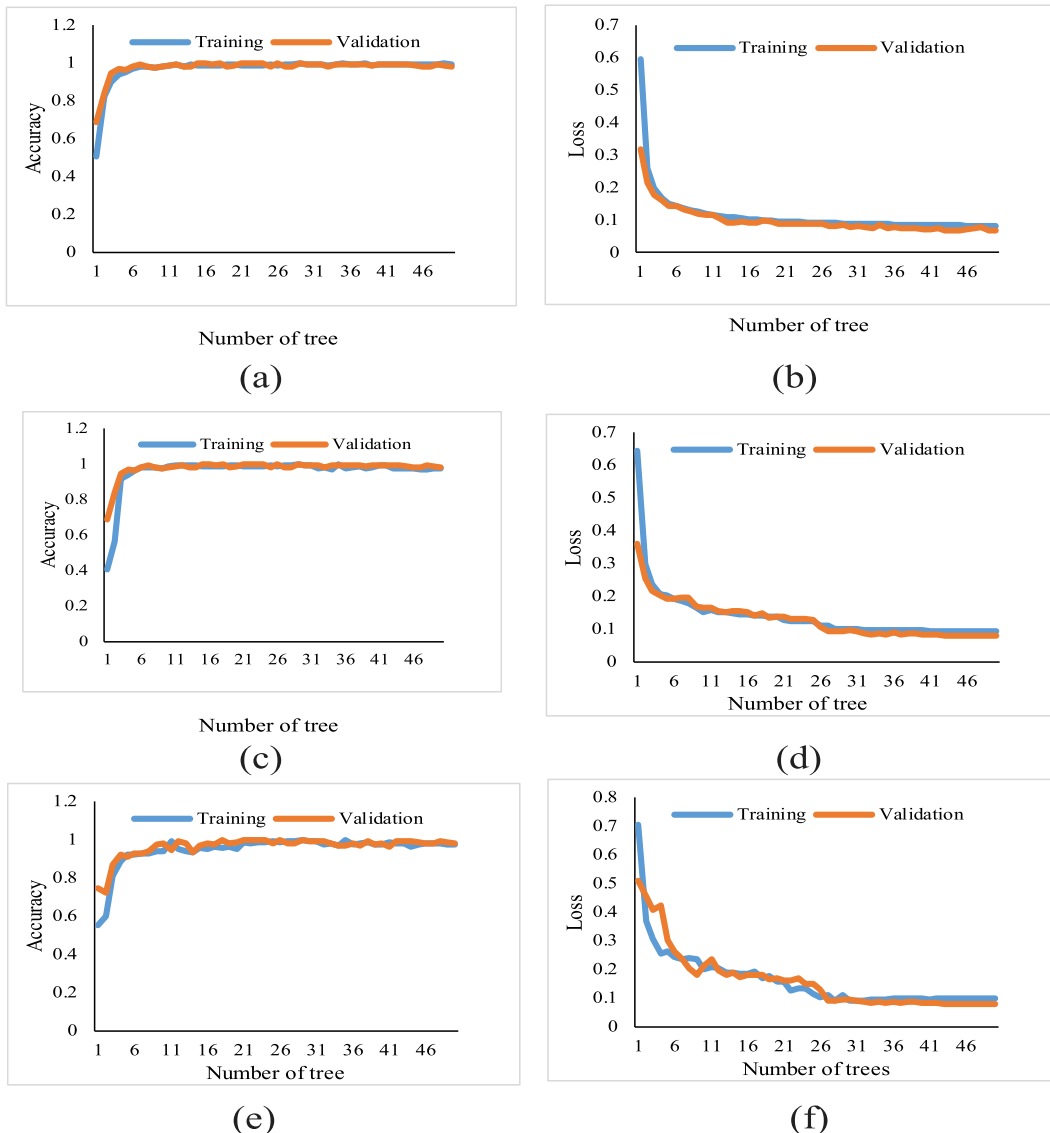


Fig. 10. Average accuracy vs average loss with respect to the number of tree. (a),(b) the experimental analysis of the training process of the proposed model using different number of cases from Bonn EEG dataset, (c) UCI-EEG dataset.

5.7. Analysis of Explainable Artificial Intelligence (XAI) for EEG epileptic seizure detection

In this subsection, we explain the interpretation of the decision making process of the base model (decision tree classifier) using the experimental type of each dataset through XAI. We used SHAP, a game theory approach, to explain the decision-making process of the models, as demonstrated by the various SHAP decision plots. These visualizations include the Summary Plot (SP) and Waterfall Plot (WP). The SP plot is illustrated in Fig. 14 (a), (b) and Fig. 15 (a) providing a global interpretation of the model of the Bonn and UCI-EEG dataset of different experiment types.

The plot shows the feature's importance with respect to classification performance, revealing the influence of each global feature on the model's outcome. The eigenvalue feature HFD_4,HFD_1 in experimental type (CD, E) and (AB,CD,E) of Bonn and HFD_4 and std_1 for UCI EEG experimental types have large absolute SVs that are identified as significant due to their higher average impact on the model's output.

Fig. 14 (c) , (d) and **Fig. 15 (b)** shows the WP plot for the Bonn and UCI cases, highlighting the behavior of True Positives (TP), False Positives (FP), False Negatives (FN), and True Negatives (TN). The WP plot uses red and blue bars to indicate features that contribute to the overall classification score, with the ability to either decrease or increase the score. Moreover, **Fig. 16 (a) to (d)**, presents the SHAP dependence plot which describes the relationship between two eigenvalue features of the STD and FD-NL and the effect on their model performance. In the plot, the x-axis represents the primary feature while the y-axis on the left side represents the secondary feature and the second y-axis on the right side represents the Shape values. In plots (a), (b), (c), and (d), the primary and secondary features across multiple domains show an increase as the shape value increases, indicating a positive correlation with the predicted outcome. From all the visualizations, it becomes evident that HFD_1 , HFD_4 play the most significant role in distinguishing between EEG states using each dataset, while PFD_3 eigenvalue feature is the least important in EEG epileptic seizure detection.

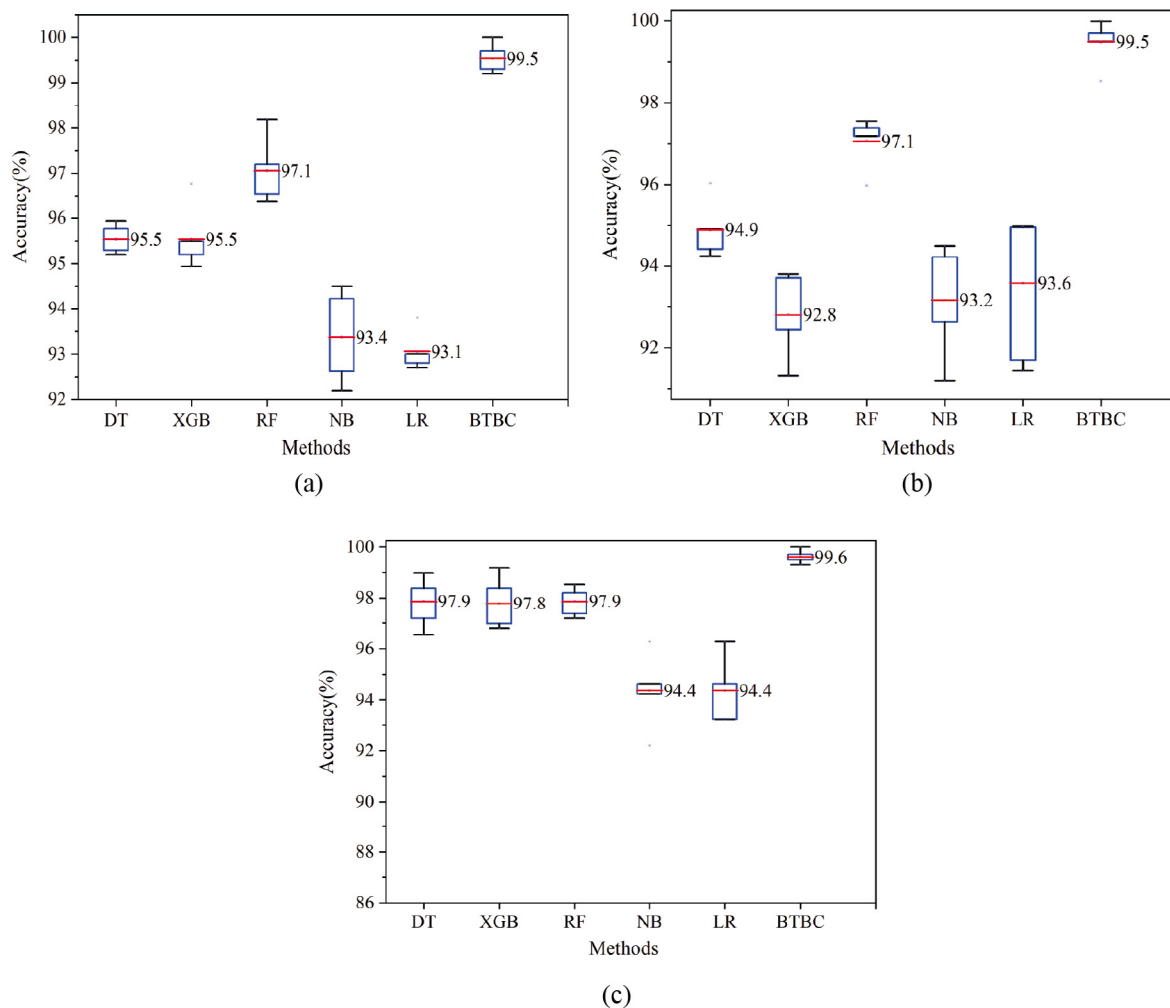


Fig. 11. Comparative results of the proposed model with recent ML models using FD-nonlinear and linear feature. (a),(b) presents the 5-fold cross validation of the Bonn , and (c) UCI-EEG dataset.

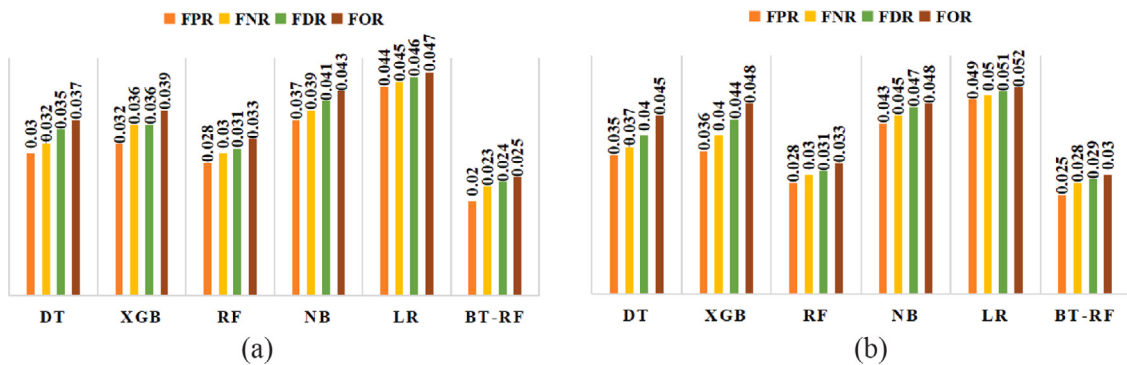


Fig. 12. The analysis based on FDR, FNR, FOR, and FPR of the proposed model in EEG epileptic seizure detection. (a) using the experiment type of Bonn, and (b) UCI-EEG data set.

6. Discussion

Epileptic seizure presents significant challenges in healthcare technology [1]. This is primarily due to the complex and non-linear nature of EEG signals, as well as the influence of various factors on seizure activity. Conventional seizure detection methods often fall short

of accurately representing the dynamic proposed nature of the EEG signals.

Furthermore, selecting the optimal features for EEG epileptic seizure detection within an automated system poses an additional challenge. The aim is to enhance classification performance by identifying the

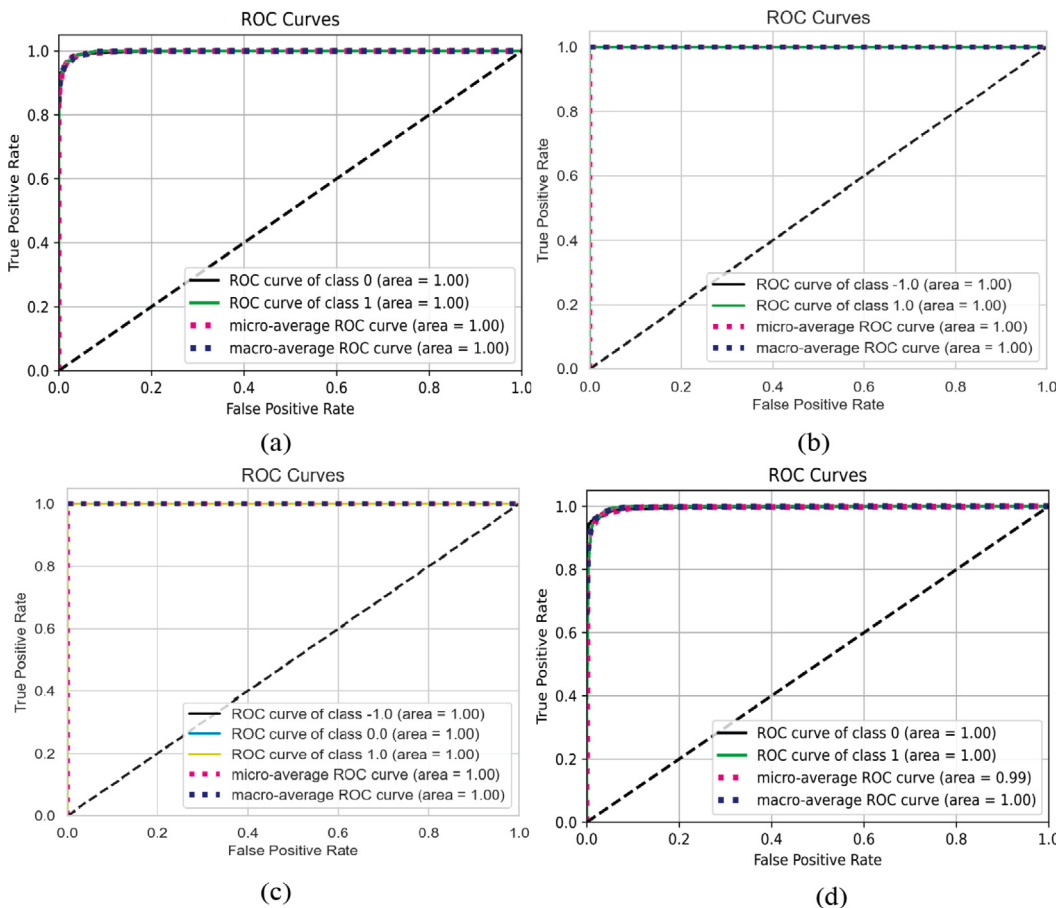


Fig. 13. The ROC curve of the proposed model using different experiment type of (a),(b),(c) Bonn, and (b) UCI-EEG data set.

Table 9

The comparative results of the proposed model with state-of-the-art methods using the Bonn EEG dataset.

Publication	Segment, sample	Experiment type	Methods	Explainability	ACC (%)	Time complexity (sec)
[34]	N/A,4097	(ABCD, E), (AB, CD, E)	TQWT +Entropy feature+PCA+ SVM	N/A	99	N/A
[17]	N/A,4097	(C-E) , (D-E)	CWT + Wavelet features + SVM,NB	N/A	97.96	N/A
[35]	N/A,4097	(AB,CD,E)	DTCWT + ST + CVNN	N/A	98	90
[36]	N/A,4097	(C, E) and (D, E)	DWT, Windowing+ ST + LSTM	N/A	97	N/A
[37]	N/A,4097	(CD,E)	Normalization + DNN Model	N/A	95.16	N/A
[38]	N/A,4097	(CD,E)	FLP + PEE, Energy + SVM	N/A	97.17	N/A
This work	8600,1338	(CD,E),(AB,CD,E)	DWT + STD and FD-NL, + CC and DC + BTBC	XAI	99.50,99.50	35

DTCWT, Dual-tree complex wavelet transform; TQWT, Tunable Q wavelet transform; CVNN, Complex value neural networks; CC, correlation coefficient; DC, distance correlation; ST, statistical features.

most informative features. Choosing effective features and ML models is essential to improve accuracy and sensitivity in ES detection compared to other methods. Moreover, ensuring model explainability and interpretability in the proposed decision-making process presents further challenges [9,10,29–33]. To the best of the authors' knowledge, no prior research has employed the correlation coefficient and distance correlation for linear and nonlinear feature selection, the Bagged Tree-based classifier and the model's explainability and interpretability through explainable AI, which includes both global and local explanations.

In addressing the challenges of EEG epileptic seizure detection, the proposed study presents a comprehensive framework that integrates various components, which includes EEG signal decomposition, noise mitigation, statistical time domain (STD) linear feature, and Fractal Dimension-based (FD) non-linear feature, with innovative feature selection methods. The proposed Bagged Tree-based classifier

effectively addresses over-fitting issues and enhances interpretability through Explainable Artificial Intelligence (XAI).

Performance evaluations using the Bonn and UCI-EEG datasets validate the effectiveness of the proposed framework. The results Fig. 9 indicate optimal performance at a correlation coefficient (CC) value of 0.82, beyond the proposed threshold, even increases in CC did not improve accuracy. Therefore, the CC value of 0.82 serves as the threshold for the model's learning and streamlines feature selection. The proposed framework incorporates FD-based linear and non-linear features extracted through wavelet decomposition. The approach uses both the linear and complex features of EEG signals, thereby enhancing the model's discrimination capacity. Comparison with various machine learning models (DT, RF, XGB, LR, NB) via 5-fold cross-validation demonstrates the superior performance of the proposed model. The bagged tree-based classifiers consistently outperform other ML models using the experimental types of the Bonn and UCI-EEG datasets

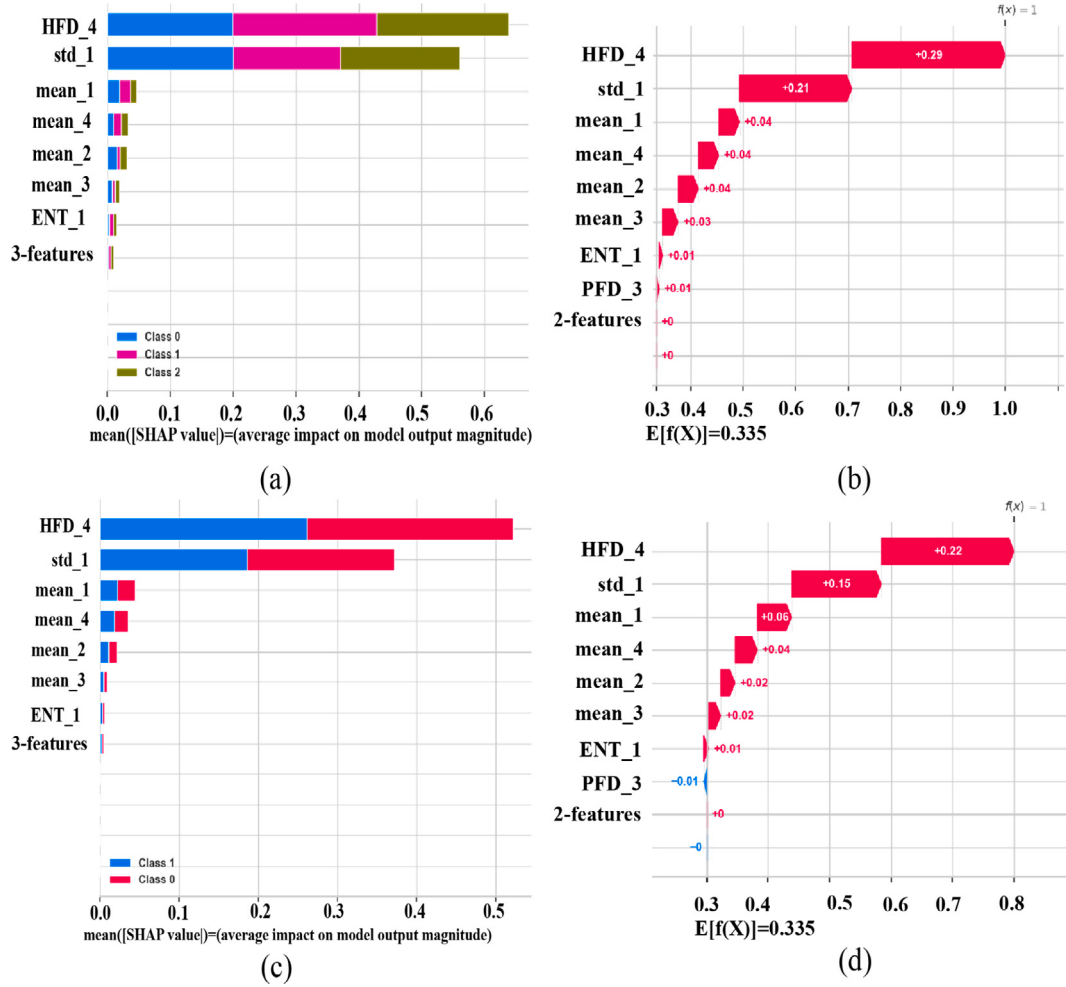


Fig. 14. Visual explanation for the propose model based on different visualizations for binary and multi-class tasks using the Bonn EEG dataset. Subfigures (a) and (c) represent summary plots, while (b) and (d) shows waterfall plots.

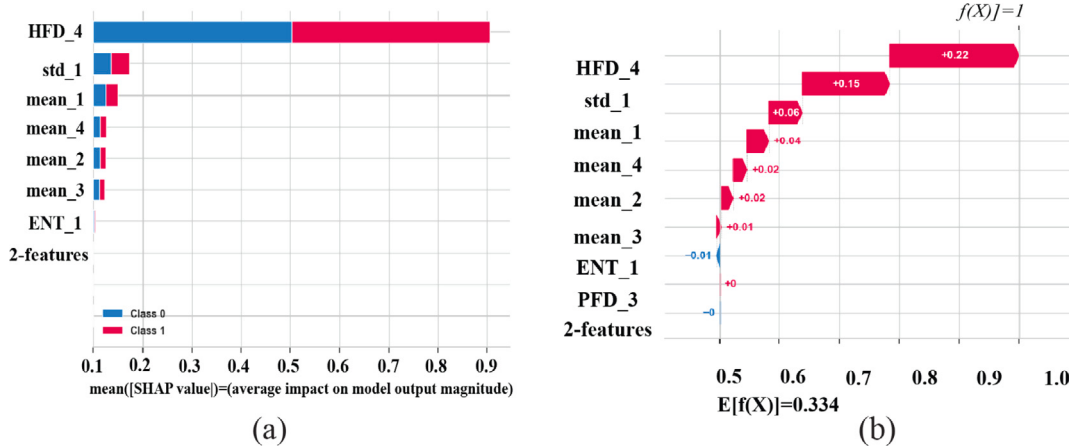


Fig. 15. The explainability of the proposed model based on different visualizations for the binary class using the UCI-EEG dataset. Subfigure (a) represents the summary plot, while (b) depicts the waterfall plot.

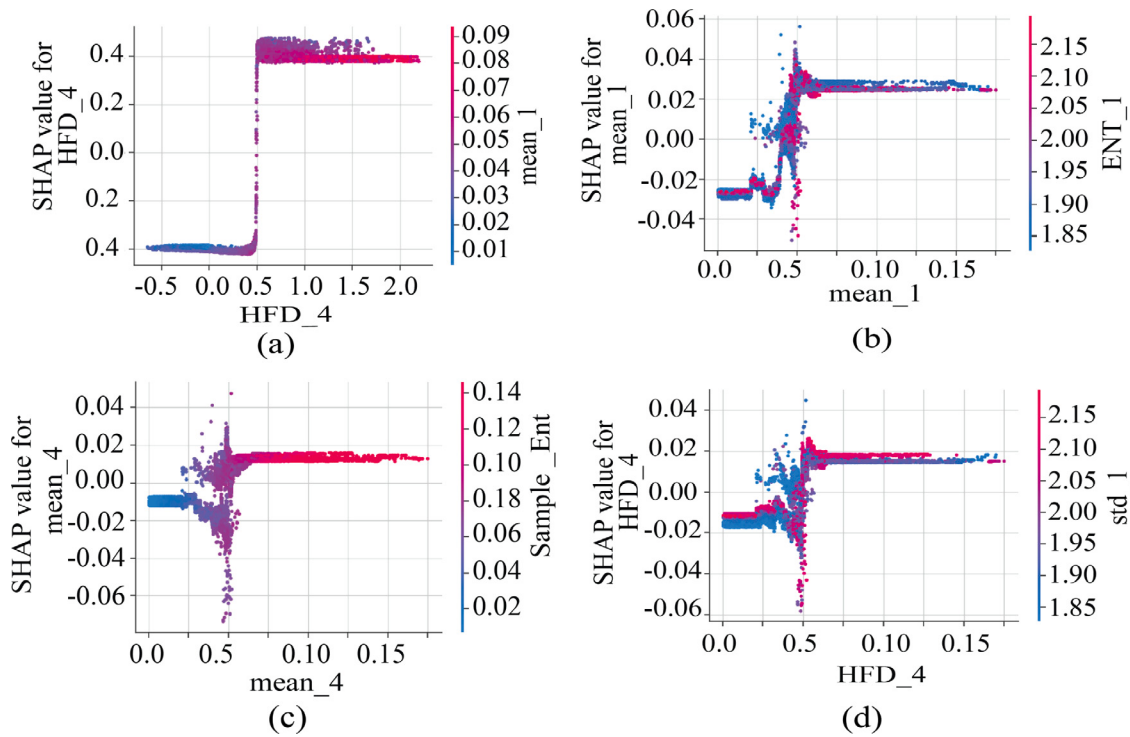


Fig. 16. Shows the Dependency plot, each subplot (a,b,c,d) represents a different features impact on the model output, with the color intensity indicating the features SHAP value using different experiment type type of the bonn and UCI EEG dataset.

Table 10

The comparative results of the proposed model with state-of-the-art methods using the experimental type of UCI EEG dataset.

Publication	Sample method	Experiment type	Methods	Explainability	ACC (%)	Time complexity (sec)
[39]	Event based	(A,B)	FT +178 features +SVM, KNN, ANN	N/A	97,96, 95	N/A
[40]	Event based	(A,B)	DCPA-EZ + DCPA-EZ	NA	98.10	N/A
[41]	Event based	(A,B)	178 features +SVM, KNN, ANN, LDA	N/A	95, 96.40, 93, 94	N/A
[42]	Event based	(A, B)	FFT + wavelet features + SOM-RBFnn	N/A	97.40	N/A
[43]	Event based	(A,B)	FFT+ 178 features+ NAMLP, ANN, SVM	N/A	94, 93, 92	N/A
This work	Event based	(A,B)	DWT + STD and FD-NL, + CC and DC + BTBC	XAI	99.60	19

showing the effectiveness of the proposed model. The model used the selected non-linear and STD linear features, effectively distinguishing the ictal, preictal, and interictal EEG states. The proposed model performance is bench-marked against recent state of art methods validated by Bonn and UCI- EEG datasets. **Table 9** and **Table 10** shows consistently outperformed existing subling models.

Explainable AI (XAI) through SHAP presents the interpretation of the proposed model decision-making process to medical experts. Summary and Waterfall Plots highlight the important features and their contributions to classifications. The proposed methods not only enhancing the accuracy but also explaining the decision-making process, which is a key advantage in healthcare settings where understanding model decisions is crucial. The high precision, sensitivity, and accuracy of the proposed framework highlight its potential for healthcare professionals in diagnosing seizures. The comprehensive understanding of EEG signals, improved feature selection through optimized correlation coefficients, robust overfitting mechanism by the model, and transparent decision-making via SHAP collectively contribute to informed decision-making, enhancing patient care and outcomes in epilepsy management. However, the proposed framework has limitations of the patient-specific approach. In future studies, our goal is to apply the framework for patient-independent, use more clinical datasets.

7. Conclusion

In this study, we introduce an automatic EEG epileptic seizure detection framework that employs novel feature selection methods, a Bagged Tree-based classifier, and Explainable Artificial Intelligence . Initially, the pre-processing of EEG signals used a Butterworth filter to reduce the noise and artifacts. Then, discrete wavelet transform based decomposition was applied, and statistical time-domain linear and FD-nonlinear features were extracted from each decomposition level. Then novel correlation coefficients for linear features and distance correlations for non-linear features were used to enable effective feature selection, improving the model's performance in EEG epileptic seizure detection. The model exhibits the best performance metrics in accuracy, precision, sensitivity, and f1-score, effectively addressing the over-fitting issue. Validation through the Bonn and UCI EEG benchmark datasets confirms the model's robustness and reliability in detecting epileptic seizures. The important aspect of the proposed framework is the implementation of XAI, achieved through SHapley Additive Explanations, which interprets the model's decision-making process, and explains the impact of each feature on the model's output. The future study will focus on patient-independent multimodel data using the proposed framework with explainability and interpretability to facilitate the clinical decision-making process in epilepsy management.

CRediT authorship contribution statement

Ijaz Ahmad: Conceptualization, Methodology, Software, Validation, Resources, Data curation, Writing – original draft, Visualization, Project administration. **Chen Yao:** Conceptualization, Visualization. **Lin Li:** Validation. **Yan Chen:** Formal analysis. **Zhenzhen Liu:** Writing – review & editing. **Inam Ullah:** Methodology, Writing – original draft. **Mohammad Shabaz:** Software, Writing – original draft. **Xin Wang:** Validation, Project administration. **Kaiyang Huang:** Writing – review & editing. **Guanglin Li:** Visualization. **Guoru Zhao:** Investigation, Writing – review & editing, Supervision, Project administration. **Oluwarotimi Williams Samuel:** Investigation, Supervision. **Shixiong Chen:** Resources, Data curation, Supervision, Funding acquisition.

Declaration of competing interest

The authors declare no conflict of interest.

Data availability

Data will be made available on request.

Acknowledgments

This work was supported in part by the National Key R&D Program of China (2022YFE0197500), National Natural Science Foundation of China (#81927804, #62101538), Science and Technology Planning Project of Shenzhen (#JSGG20210713091808027, #JSGG20211029095801002), China Postdoctoral Science Foundation (2022M710968), the Science and Technology Program of Guangdong Province (2022A0505090007).

References

- [1] Spagnoli C, Fusco C, Pisani F. Rett syndrome spectrum in monogenic developmental-epileptic encephalopathies and epilepsies: A review. *Genes* 2021;12(8):1157.
- [2] Pati S, Alexopoulos AV. Pharmacoresistant epilepsy: from pathogenesis to current and emerging therapies. *Cleve Clin J Med* 2010;77(7):457–567.
- [3] Obeidat MA, Mansour AM. EEG based epilepsy diagnosis system using reconstruction phase space and Naïve Bayes classifier. *WSEAS Trans Circuits Syst* 2018;17.
- [4] WHO. Epilepsy care. 2022, Available online: <https://www.who.int/mental-health>, (accessed December 7, 2022).
- [5] Subasi A, Kevric J, Abdullah Canbaz M. Epileptic seizure detection using hybrid machine learning methods. *Neural Comput Appl* 2019;31:317–25.
- [6] Abdulbaqi AS, Younis MT, Younus YT, Obaid AJ. A hybrid technique for EEG signals evaluation and classification as a step towards to neurological and cerebral disorders diagnosis. *Int J Nonlinear Anal Appl* 2022;13(1):773–81.
- [7] Ahmad I, Wang X, Zhu M, Wang C, Pi Y, Khan JA, et al. EEG-based epileptic seizure detection via machine/deep learning approaches: A systematic review. *Comput Intell Neurosci* 2022;2022.
- [8] Ijaz Ahmad X, Javeed D, Kumar P, Samuel OW, Chen S. A hybrid deep learning approach for epileptic seizure detection in EEG signals. *IEEE J Biomed Health Inf* 2023.
- [9] Tjoa E, Guan C. A survey on explainable artificial intelligence (xai): Toward medical xai. *IEEE Trans Neural Netw Learn Syst* 2020;32(11):4793–813.
- [10] Raab D, Theissler A, Spiliopoulou M. XAI4EEG: spectral and spatio-temporal explanation of deep learning-based seizure detection in EEG time series. *Neural Comput Appl* 2022;1–18.
- [11] Al-Salman W, Li Y, Wen P, Miften FS, Oudah AY, Al Ghayab HR. Extracting epileptic features in EEGs using a dual-tree complex wavelet transform coupled with a classification algorithm. *Brain Res* 2022;1779:147777.
- [12] Kaushik G, Gaur P, Sharma RR, Pachori RB. EEG signal based seizure detection focused on Hjorth parameters from tunable-Q wavelet sub-bands. *Biomed Signal Process Control* 2022;76:103645.
- [13] Nasir IM, Khan MA, Yasmin M, Shah JH, Gabryel M, Scherer R, et al. Pearson correlation-based feature selection for document classification using balanced training. *Sensors* 2020;20(23):6793.
- [14] Aliyu I, Lim CG. Selection of optimal wavelet features for epileptic EEG signal classification with LSTM. *Neural Comput Appl* 2021;1–21.
- [15] Andrzejak RG, Lehnertz K, Mormann F, Rieke C, David P, Elger CE. Indications of nonlinear deterministic and finite-dimensional structures in time series of brain electrical activity: Dependence on recording region and brain state. *Phys Rev E* 2001;64(6):061907.
- [16] Harender B, Sharma R. DWT based epileptic seizure detection from EEG signal using k-NN classifier. In: 2017 international conference on trends in electronics and informatics (ICEI). IEEE; 2017, p. 762–5.
- [17] Sharmila A, Geethanjali P. DWT based detection of epileptic seizure from EEG signals using naive Bayes and k-NN classifiers. *Ieee Access* 2016;4:7716–27.
- [18] Uthayakumar R, Eswaramoorthy D. Epileptic seizure detection in EEG signals using multifractal analysis and wavelet transform. *Fractals* 2013;21(02):1350011.
- [19] Nijssen TME. Accelerometry based detection of epileptic seizures. 2008.
- [20] Parashar A, Parashar A, Ding W, Shabaz M. Data preprocessing and feature selection techniques in gait recognition: A comparative study of machine learning and deep learning approaches. *Pattern Recognit Lett* 2023.
- [21] Hussain SF, Qaisar SM. Epileptic seizure classification using level-crossing EEG sampling and ensemble of sub-problems classifier. *Expert Syst Appl* 2022;191:116356.
- [22] Xie L, Li Z, Zhou Y, He Y, Zhu J. Computational diagnostic techniques for electrocardiogram signal analysis. *Sensors* 2020;20(21):6318.
- [23] Nishad A. Tunable-Q wavelets transform based filter banks for non-stationary signals analysis and classification. 2019.
- [24] Upadhyay R, Manglick A, Reddy D, Padhy P, Kankar PK. Channel optimization and nonlinear feature extraction for electroencephalogram signals classification. *Comput Electr Eng* 2015;45:222–34.
- [25] Fei L, Zhang B, Xu Y, Tian C. Jointly heterogeneous palmprint discriminant feature learning. *IEEE Trans Neural Netw Learn Syst* 2021;33(9):4979–90.
- [26] Sadiq MT, Yu X, Yuan Z, Zeming F, Rehman AU, Ullah I, et al. Motor imagery EEG signals decoding by multivariate empirical wavelet transform-based framework for robust brain-computer interfaces. *IEEE Access* 2019;7:171431–51.
- [27] UML Repository, epileptic seizure recognition data set. 2022, Available online:<https://archive.ics.uci.edu/ml/datasets/Epileptic+Seizure+Recognition>, (accessed December 7, 2022).
- [28] Ji N, Ma L, Dong H, Zhang X. EEG signals feature extraction based on DWT and EMD combined with approximate entropy. *Brain Sci* 2019;9(8):201.
- [29] Goldberger AL, Amaral LA, Glass L, Hausdorff JM, Ivanov PC, Mark RG, Mietus JE, Moody GB, Peng C-K, Stanley HE. Physiobank, physiotoolkit, and physionet: components of a new research resource for complex physiologic signals. *circulation* 2000;101(23):e215–20.
- [30] Fei L, Teng S, Wu J. Enhanced minutiae extraction for high-resolution palmprint recognition. *Int J Image Graph* 2017;17(04):1750020.
- [31] Al-Qazzaz NK, Ali SHBM, Ahmad SA. Recognition enhancement of dementia patients' working memory using entropy-based features and local tangent space alignment algorithm. In: Advances in non-invasive biomedical signal sensing and processing with machine learning. Springer; 2023, p. 345–73.
- [32] Mursalin M, Zhang Y, Chen Y, Chawla NV. Automated epileptic seizure detection using improved correlation-based feature selection with random forest classifier. *Neurocomputing* 2017;241:204–14.
- [33] Demirci BA, Demirci O, Engin M. Comparative analysis of ANN performance of four feature extraction methods used in the detection of epileptic seizures. *Comput Biol Med* 2023;107491.
- [34] Mardini W, Yassein MMB, Al-Rawashdeh R, Aljawarneh S, Khamayseh Y, Meqdadi O. Enhanced detection of epileptic seizure using EEG signals in combination with machine learning classifiers. *IEEE Access* 2020;8:24046–55.
- [35] Peker M, Sen B, Delen D. A novel method for automated diagnosis of epilepsy using complex-valued classifiers. *IEEE J Biomed Health Inform* 2015;20(1):108–18.
- [36] Supriya S, Siuly S, Wang H, Cao J, Zhang Y. Weighted visibility graph with complex network features in the detection of epilepsy. *IEEE Access* 2016;4:6554–66.
- [37] Akyol K. Stacking ensemble based deep neural networks modeling for effective epileptic seizure detection. *Expert Syst Appl* 2020;148:113239.
- [38] Joshi V, Pachori RB, Vijesh A. Classification of ictal and seizure-free EEG signals using fractional linear prediction. *Biomed Signal Process Control* 2014;9:1–5.
- [39] Rohan TI, Yusuf MSU, Islam M, Roy S. Efficient approach to detect epileptic seizure using machine learning models for modern healthcare system. In: 2020 IEEE region 10 symposium (TENSYMP). IEEE; 2020, p. 1783–6.
- [40] Hilal AM, Albraikan AA, Dhahbi S, Nour MK, Mohamed A, Motwakel A, et al. Intelligent epileptic seizure detection and classification model using optimal deep canonical sparse autoencoder. *Biology* 2022;11(8):1220.
- [41] Almustafa KM. Classification of epileptic seizure dataset using different machine learning algorithms. *Inform Med Unlocked* 2020;21:100444.
- [42] Osman AH, Alzahrani AA. New approach for automated epileptic disease diagnosis using an integrated self-organization map and radial basis function neural network algorithm. *IEEE Access* 2018;7:4741–7.
- [43] Shankar RS, Raminaidu C, Raju VS, Rajanikanth J. Detection of epilepsy based on EEG signals using PCA with ANN model. *J Phys: Conf Ser* 2021;2070(1):012145.